Research Paper

The Role of Tear faults on the Morphology and Seismic Activity of the Ashkhaneh Fault Zone, Kopeh-Dagh, NE Iran

Saeid Rahimzadeh[1*] and Noorbakhsh Mirzaei[2]

1. Ph.D. Student, Institute of Geophysics, University of Tehran, Tehran, Iran,
*Corresponding Author; email: saeid.rahimzadeh@ut.ac.ir
2. Professor, Institute of Geophysics, University of Tehran, Tehran, Iran

Received: 27/05/2023
Revised: 04/07/2023
Accepted: 10/07/2023

ABSTRACT

The Kopeh-Dagh zone of NE Iran is dominated by active strike-slip and thrust faults that accommodate a part of the convergence between the Arabian and Eurasian Plates. The Ashkhaneh thrust fault zone with approximately 80 km long is one of the main accommodative structures, which has been dissected by a number of strike-slip tear faults. Tectonic geomorphology, satellite-based Global Positioning System (GPS), and seismic data imply that the development of tear faults is one of the main controlling factors in structural deformation and related seismic activity along the Ashkhaneh thrust fault zone. The tectonic activity of the Ashkhaneh fault zone is mainly due to the E-W trending range-parallel reverse faults and NE-SW to ENE-WSW trending range-crossing left-lateral strike-slip tear faults coming from two stages. In the first stage, the major E-W trending Ashkhaneh thrust fault zone has been developed in response to the collision of Central Iran with the South Caspian Basin. In the second stage, the progressive N-S shortening resulted in mountain curvature in eastern Alborz and the formation of strike-slip tear faults in response to the differential shortening along the Ashkhaneh fault zone. The sense of slip and geometry of the tear faults and the Ashkhaneh thrust fault seems to provide insights into faults interaction, so that the likely movement along one of these faults may cause reactivation of the other fault(s); similar to the earthquake occurrences on the Shalgun-Yelimsi tear fault (2019/11/07, Mw 5.9) and South Bozgush thrust fault (2019/11/10, Mw 4.4) in northwestern Iran.

Keywords:
Active tectonics; Tear fault, Faults interaction; Ashkhaneh fault zone; Kopeh-Dagh; Northeast Iran

1. Introduction

Tear faults are relatively small-scale local strike-slip faults, commonly subsidiary to other structures such as folds and thrust faults (Twiss & Moores, 2007; Qingfen et al., 2008; Yong, 2010; Yong et al., 2014). In terms of geometry, tear faults are steeply dipping (or near vertical) shear zones sub-parallel to the regional direction of displacement which accommodate different amounts of crustal lengthening or shortening in adjacent regions (Twiss & Moores, 2007; Qingfen et al., 2008; Yong, 2010; Yong et al., 2014; Lin et al., 2011) (Figure 1).

Thrust sheets are not structurally continuous features; instead, they are divided (or segmented) by tear faults, which accommodate the differential displacement of different parts of the sheet, or connect parts of the active thrust that are not coplanar (Figure 1) (Twiss & Moores, 2007). Tear faults likely connect en-echelon thrusts at depth and transfer stress among them (Lin et al., 2011). This study focuses on the role of tear faults on the morphology and seismic activity of the Ashkhaneh (Takal-Kuh) fault zone in northeast Iran (Figure 2). Ashkhaneh fault is a thrust fault zone with a slight sinistral motion that is extended about 80 km in the western Kopeh-Dagh mountain belt (Figure 2). Visible changes in the strike of this fault zone, imply that morphological responses to tectonic activities should be different along the fault. Here, we describe and discuss the significance

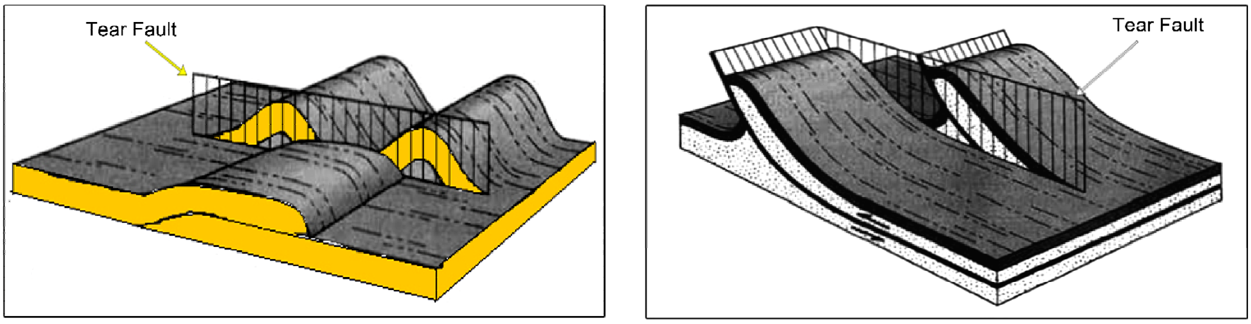

(a) Shortening Is Accommodated by Folding on One Side of a Strike-Slip Tear fault and by Thrusting on the Other

(b) Two Non-Coplanar Imbricate Thrusts Connected by a Strike-Slip Tear Fault (After Twiss & Moress, 2007)

Figure 1. Thrust sheets segmented by strike-slip tear faults.

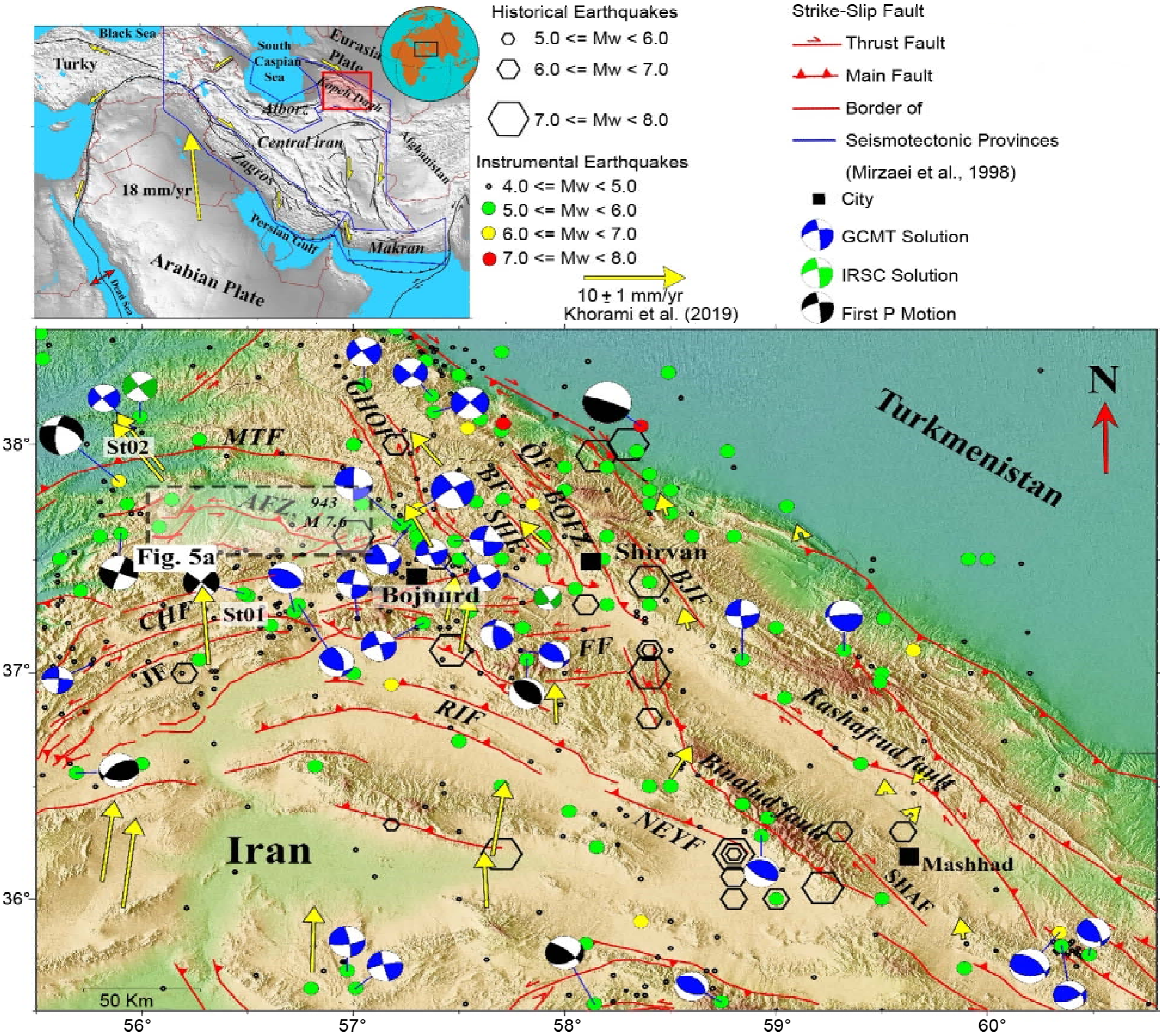

Figure 2. Active faulting in northeastern Iran. Our study area is outlined by the red rectangle on the index map. Black, blue, and green focal mechanisms are from Mirzaei et al. (2002), the Global Centroid Moment Tensor Project (GCMT), and the Iranian Seismological Center (IRSC), respectively. The epicenter of the earthquakes is from IRSC. Major faults are mainly based on Hollings worth et al. (2006, 2008, 2010), and Javidfakhr et al. (2011). AFZ: Ashkhaneh fault zone, BQFZ: Bakharden-Quchan fault zone, FF: Farhadan fault, CHF: Cheshmeh-Nik fault, NEYF: Neyshabur fault zone, RIF: Rivand fault zone, MTF: Maraveh Tappeh fault zone, SHAF: Shandiz fault zone, GHOF: Gholaman fault zone, JF: Jajarm fault zone, BF: Baghan fault, QF: Quchan fault, BJF: Bajgiran fault, SHF: Shirvan fault zone.

of the tear faulting in this zone to introduce local tectonic deformation and its related seismic processes in the context of the Arabia-Eurasia collision. An important by-product of this work is introducing the rule of tear faults in the seismic hazard of the region.

2. Tectonic Setting and Seismicity

2.1. Regional Tectonic

The Kopeh-Dagh mountain range of northeastern Iran, as a part of the Alpine-Himalayan Mountain belt in western Asia, is located at the eastern corner of the Arabia-Eurasia collision zone (Jackson et al., 1995) (Figure 2). It represents up to 10 km thick Mesozoic and Tertiary sediments, deposited in a subsiding basin during the Mesozoic extensional regime, which were folded during the last phase of the Alpine orogeny (Tchalenko, 1975; Berberian, 1981). The Kopeh-Dagh and Binalud mountain ranges together form a mountain belt of about 600 km long and about 200 km wide forming the Kopeh-Dagh major seismotectonic province (Figure 2) (Mirzaei et al., 1998). The present-day kinematics of northeast Iran is characterized by a northward motion with respect to Eurasia, whose amplitude decreases linearly toward the eastern and northern borders of Iran (Figure 2) (Vernant et al., 2004; Hollingsworth et al., 2008). Based on geodetic GPS measurements (Vernant et al., 2004), the accommodation of Arabia-Eurasia plate convergence within the Kopeh-Dagh region occurs with a present-day shortening rate of 6.2±2 mm yr^{-1}. Faulting in this region includes NNW-SSE right-lateral and ENE-WSW left-lateral strike-slip, and E-W thrust-slip motion (Hollingsworth et al., 2006, 2008, 2010; Shabanian et al., 2009) (Figure 2). The dominance of strike-slip faults in the Kopeh-Dagh region, between 57-59°E, is a result of block rotation (Hollingsworth et al., 2008, 2010) (Figure 3). The zone

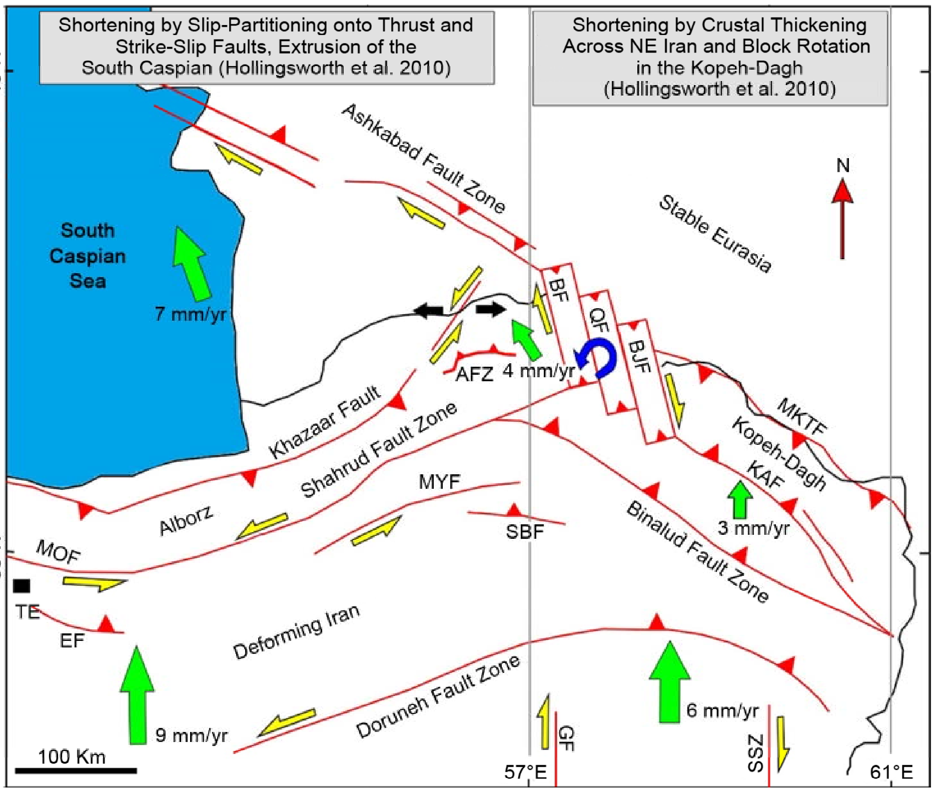

Figure 2. Simplified summary tectonic map of northeastern Iran modified from Hollingsworth et al. (2010). Faults are shown in red. Anticlockwise rotating blocks (blue arrow) of the Central Kopeh-Dagh are shown schematically (Hollingsworth et al., 2006, 2010). Green arrows and their associated values show approximate northward velocities across NE Iran (mm/yr), relative to Eurasia, based on the GPS measurements. Shortening across the Kopeh-Dagh is accommodated by oblique slip on range-bounding thrust faults east of 59° E, anticlockwise rotation of right-lateral strike-slip faults which cut obliquely across the range between 57-59° E, and westward extrusion of the West Kopeh Dagh block in the west of 57° E. TE: Tehran, BF: Baghan fault, QF: Quchan fault, BJF: Bajgiran fault, SSZ: Sistan Suture zone, GF: Gowk-Nayband fault system, SBF: Sabzevar fault zone, KAF: Kashafrud fault zone, MKTF: Main Kopeh-Dagh thrust fault, AFZ: Ashkhaneh fault zone, EF: Eyvanekey fault zone, MOF: Mosha fault zone, MYF: Meyamey fault zone.

of NNW-SSE right-lateral strike-slip faults and their anticlockwise rotation accommodates shortening and along strike extension (Hollingsworth et al., 2006, 2008, 2010). East of 59°E and West of 57° E N-S shortening is accommodated by range-bounding thrust faulting, and the westward extrusion of the western Kopeh-Dagh between the Shahrud fault zone and the Ashkabad fault zone, respectively (Hollingsworth et al., 2006, 2008, 2010) (Figure 3).

2.2. Seismicity

The spatial distribution of both historical and instrumental earthquakes indicates that northeastern Iran is a seismically active zone (Figure 2) (Ambraseys & Melville, 1982; Berberian & Yeats, 1999; Berberian, 2014). Northeastern Iran has witnessed destructive earthquakes of 943/08 (M_w 7.6), 1695/05/11 (M_w 7.0), 1879 (M_w 6.6), and 1997/02/04 (M_w 6.5) near Bojnurd; 1673/07/30 (M_w 6.5) in Mashhad; 1209 (M_w 7.3), 1270/10/07 (M_w 7.1), 1389/02 (M_w 7.6), 1405/11/23 (M_w 7.6) in Neyshabur; 1810 (M_w 6.4) in Gholaman; 1851.06 (M_w 6.9), 1871/12/23 (M_w 7.2), 1893/11/17 (M_w 7.1), and 1895/01/17 (M_w 6.8) near Quchan and 1929/05/01 (M_w 7.2) near Shirvan (Figure 2) (Ambraseys & Melville, 1982; Hollingsworth et al., 2006). A destructive earthquake in 1673/07/30 destroyed many regions of Mashhad and killed about 4000 people (Figure 2) (Ambraseys & Melville, 1982). NW-SE trending Shandiz fault has been proposed by Hollingsworth et al. (2010) as a possible source of this earthquake. Four earthquakes (1851, 1871, 1893, and 1895) that occurred near Quchan were associated with the Bakharden-Quchan fault zone and killed more than 8000 people (Tchalenko, 1975; Ambraseys & Melville, 1982). The 1929 destructive major earthquake (Mw 7.2) with a coseismic ground rupture length of more than 50 km along the Baghan fault caused considerable damage north and east of Shirvan and killed 3500 people (Tchalenko, 1975; Ambraseys & Melville, 1982; Hollingsworth et al., 2006) (Figure 2). The 1997 earthquake (Mw 6.5) occurred ~30 km north of Bojnurd (Figure 2), completely destroying 4200 houses, and damaging about 11,000 houses in more than 170 villages, which killed 88 and injured 1950 people (Hollingsworth et al., 2006; Berberian, 2014). The 1997 earthquake ruptured a right-lateral strike-slip fault, with a strike similar to Quchan and Shirvan faults (Hollingsworth et al., 2006) (Figure 2). The most recent major earthquake that occurred in the region, was the 2017/04/05, M_w 6.1, that occurred in the Kashafrud thrust fault located (Figure 2) (Ghayournajarkar & Fukushima, 2020; Prajapati & Mishra, 2021). The spatial distribution of earthquakes shows that moderate and large magnitude earthquakes ($M \geq 5.0$) have been concentrated along major fault zones such as the Binalud, Bakharden-Quchan, and Neyshabur fault zones (Figure 2). Most of the focal mechanism solutions of earthquakes in the region indicate strike-slip faulting (Figure 2). They are associated with the NNW-SSE trending right-lateral faults and ENE-WSW trending sinistral faults. There are also a few mechanisms showing reverse motion associated with the eastern part of the Cheshmeh-Nik fault zone and the southern end of the Kashafrud fault zone. Based on the Global Centroid Moment Tensor (GCMT) solutions, the centroid depth of earthquakes ranges from 15 to 20 km (https://www.globalcmt.org/).

No earthquakes with $M \geq 5.0$ have been recorded along the Ashkhaneh fault zone (Figure 2), but local networks of the Iranian Seismological Center (http://irsc.ut.ac.ir) have recorded a considerable number of small ($M < 5.0$) earthquakes along and in the vicinity of the fault zone since 2006 (Figures 2 and 4). Ambraseys and Melville (1982) point to a historical earthquake with an estimated magnitude of 7.6 near the eastern tip of the Ashkhaneh fault in 943 (Figure 2). This earthquake killed 5000 people and more than 30 villages were affected by landslides and ground deformation in the Samalqan region of North Khorasan province (Ambraseys & Melville, 1982).

3. Ashkhaneh Fault Zone

The E-W to NW-SE trending Ashkhaneh fault zone, with ~ 80 km length, located in the western part of Ashkhaneh town of North Khorasan province, is one of the most important thrust fault zones of the western Kopeh-Dagh mountain range (Figures 2 and 5a) (Javidfakhr et al., 2009,

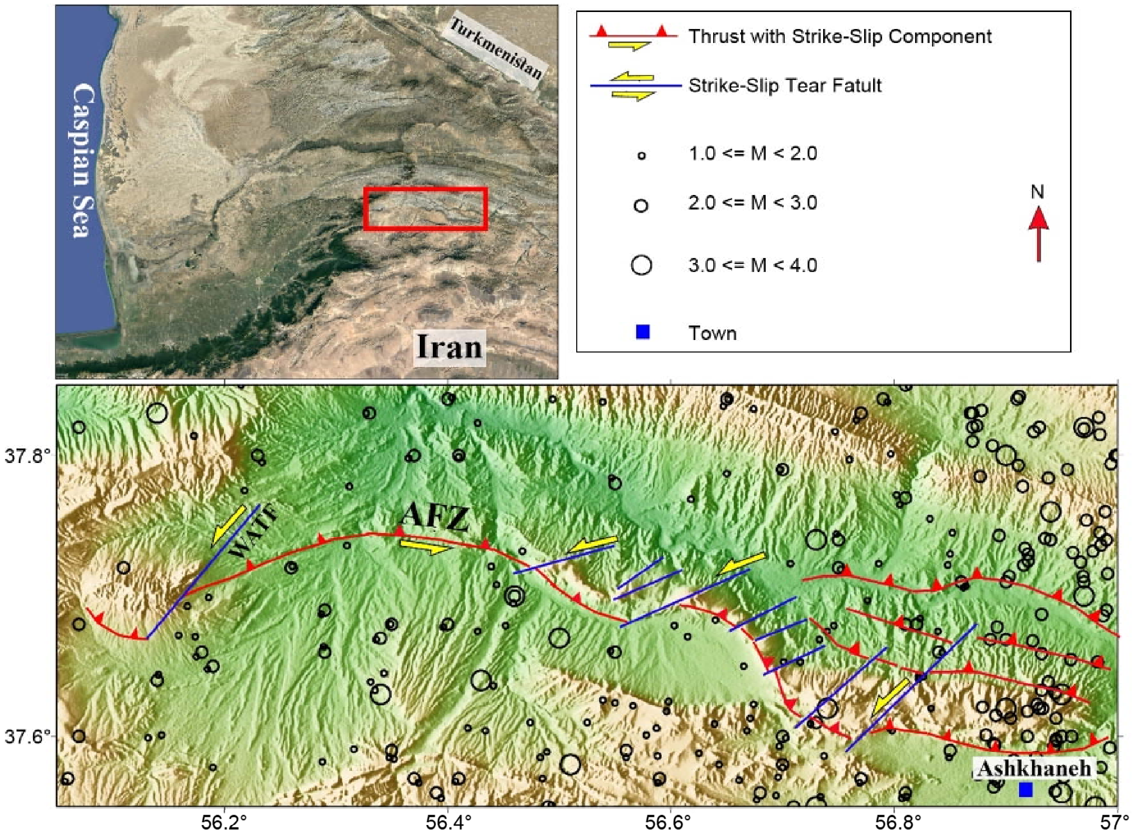

Figure 4. Epicenter distribution map of earthquakes recorded by IRSC from 2006 to 2022. WATF: West Ashkhaneh tear fault, AFZ: Ashkhaneh fault zone.

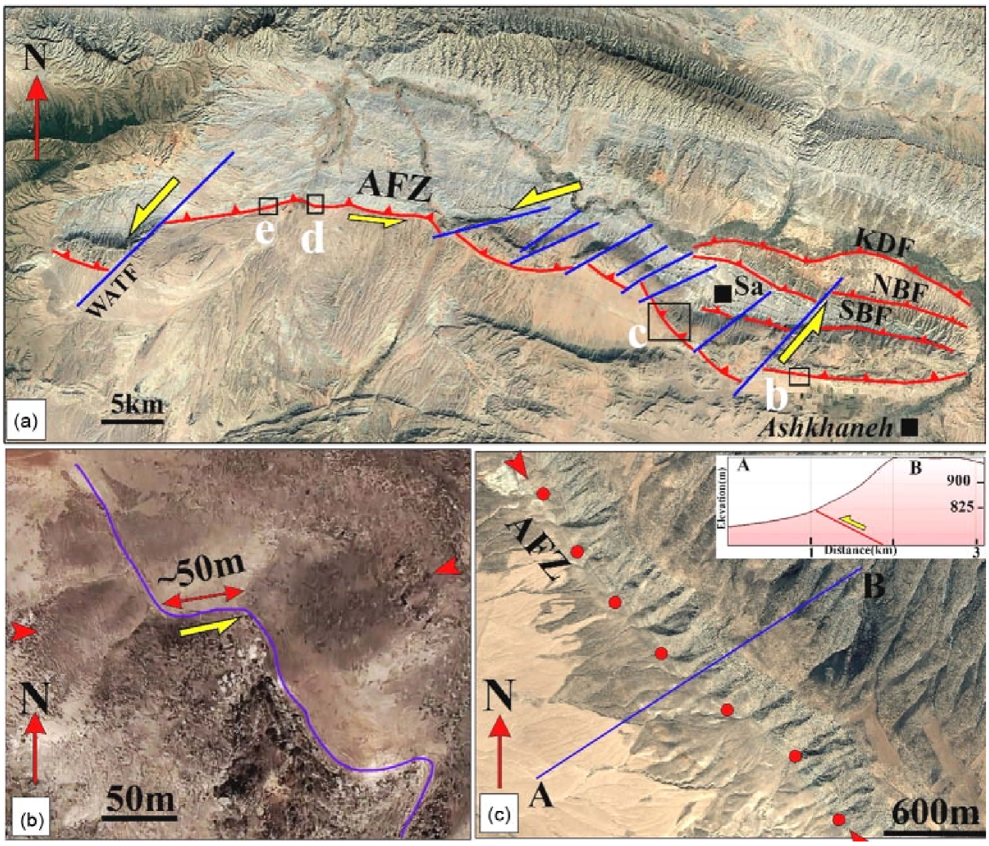

Figure 5. (a) Google Earth satellite imagery of the Ashkhaneh fault zone (AFZ). See also Fig. 2 for the location. Black quadrangles indicate the sites with observed left-lateral strike-slip displacement. (b-e) Google Earth satellite images, showing left-lateral displacement. The inset in Figure 5c shows the topographic profile across the fault. Red circles and red arrows represent the AFZ trace. WATF: West Ashkhaneh tear fault, KDF: Kuh-e-Docheng fault, NBF: North Beruj fault, SBF: South Beruj fault, Sa: Samalqan.

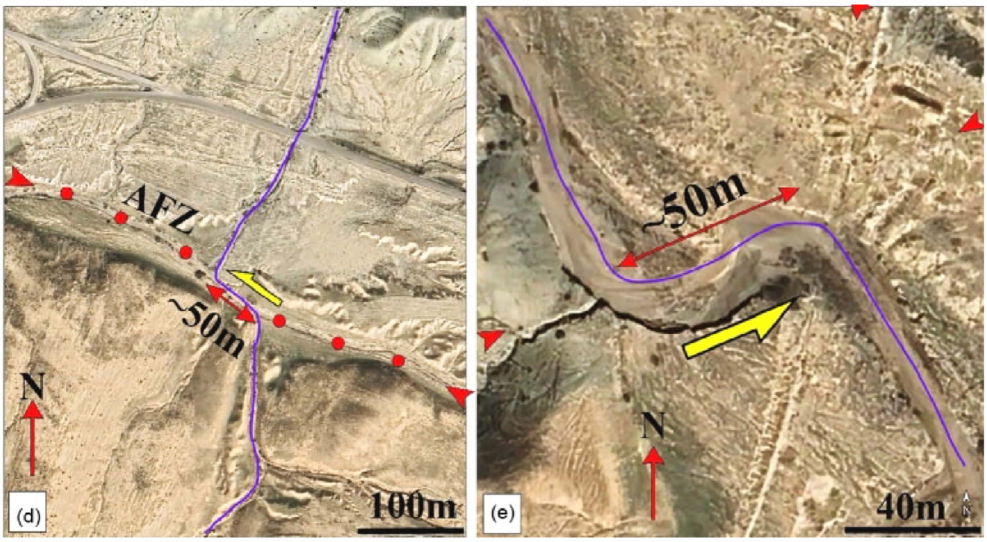

Figure 5. Continue.

2011; Bretis et al., 2012). According to Bretis et al. (2012), part of the Miocene to recent N-S shortening between Iran and Eurasia has been accommodated along the Ashkhaneh fault zone. Geomorphic and geologic features along the Ashkhaneh fault exhibit both lateral and vertical offsets along the fault (Javidfakhr et al., 2009, 2011). Javidfakhr et al. (2011) indicated a trans-pressional tectonic regime (with an N036±20°E trending horizontal ?1) along the trace of the Ashkhaneh fault zone. Bretis et al. (2012) introduced the Ashkhaneh fault zone as an oblique thrust with a number of sinistral strike-slip tear faults which accommodate the N-S shortening between Iran and Eurasia and the W-E extension of the Western Kopeh-Dagh towards the South Caspian Sea. Based on stereographic analysis of the measured structural elements and constructing cross-sections, Gholami et al. (2017) showed a dominant reverse mechanism with the sinistral strike-slip component for the Ashkhaneh fault zone; as well as the migration of rock units toward the south-southwest in this area. To the east and in the hanging-wall of the Ashkhaneh fault zone, several thrust faults such as the Kuh-e-Docheng fault, North Beruj fault, and South Beruj fault have geometrical characteristics similar to the fault zone (Gholami et al., 2017) (Figure 5a).

The Ashkhaneh fault marks a distinct topographic boundary between mountainous regions (to the north) and low-land plains to the south (Figures 5a, 5c). Uplifted surfaces, left laterally offset streams, and deflected rivers along the fault zone are the most significant morphological markers of active faulting (Figure 5b-5e). Left-lateral offsets as large as ~50 m have been documented along the fault zone (see Figures 5b, 5d, and 5e). If this left-lateral offsets date from the last major regional incision event, found to be 12 ± 2 ka in eastern Iran (Fattahi et al., 2006), as assumed by Hollingsworth et al. (2008), to estimate the slip rate on the Astaneh fault in eastern Alborz, this would indicate a slip rate of 3-5 mm/yr on the Ashkhaneh fault. The observed 50 m offset may imply large earthquakes have probably occurred on the Ashkhaneh fault zone during the Holocene. However, these estimates are very simple.

NE-SW to ENE-WSW trending tear faults are visible along the Ashkhaneh fault zone, both in the field geological exploration results (Bretis et al., 2012) and on the satellite images (Figure 6a). These tear faults which play a very important role in separating structural units are steep and cut through deeper (Xue et al., 2021). These tear faults, with 5 to 25 km length, are mainly seen in the eastern part of the Ashkhaneh fault zone (Figure 6a). Left-lateral displacements on these tear faults are variable, ranging from 150 to 1100 m (Figures 6b-6g). The westernmost part of the Ashkhaneh fault zone has been dissected by a strike-slip tear fault (West Ashkhaneh tear fault) (Figure 6a). The NE-SW trending West Ashkhaneh tear fault is about 25 km long, located roughly

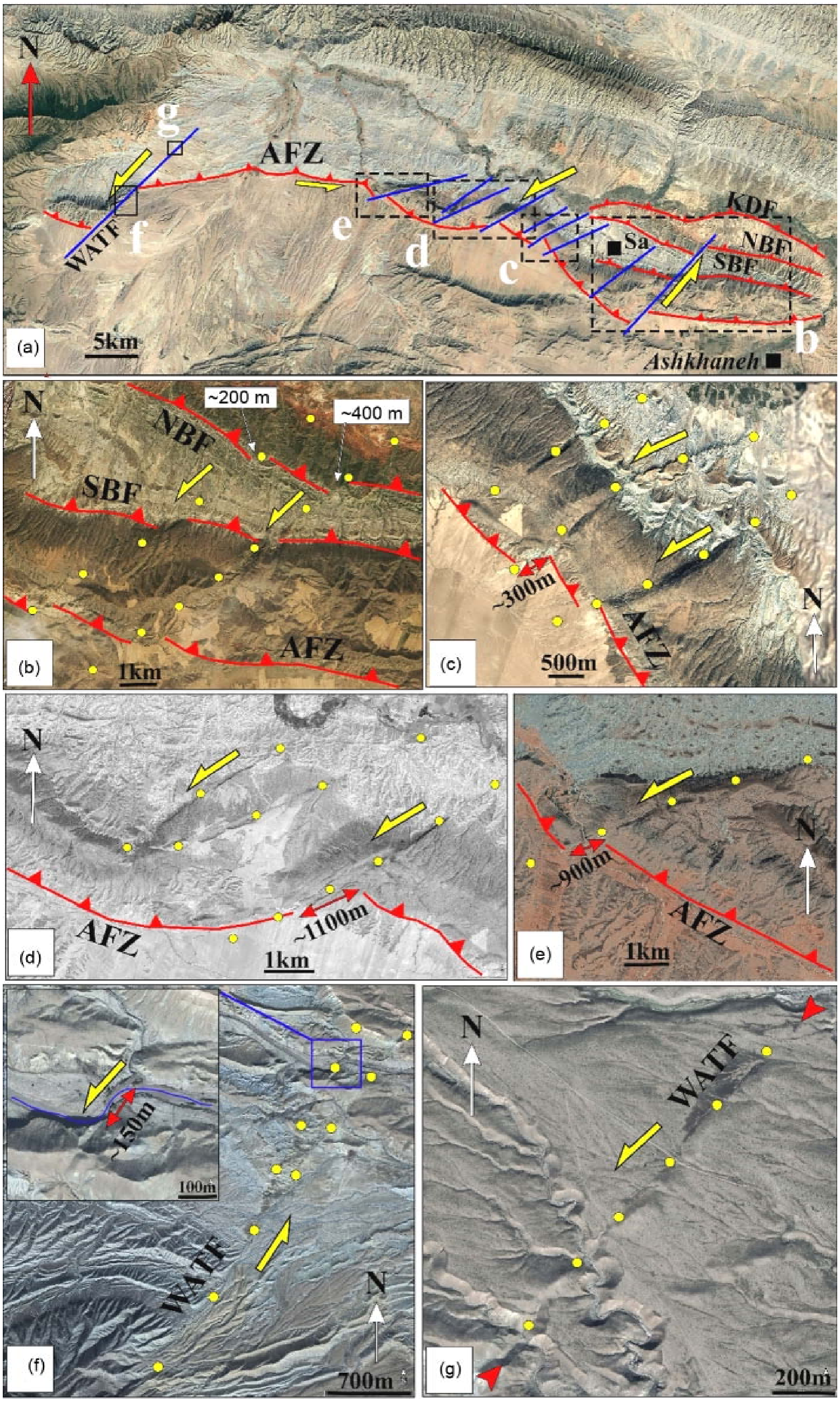

Figure 6. (a) Google Earth satellite imagery of the Ashkhaneh fault zone (AFZ). (b-e) Google Earth satellite imagery of the tear faults with left-lateral movements cut the AFZ. Yellow circles and red arrows represent the tear strike-slip fault traces. (f and g) Google Earth satellite imagery of the West Ashkhaneh tear fault (WATF). Yellow circles and red arrows represent the WATF trace. KDF: Kuh-e-Docheng fault, NBF: North Beruj fault, SBF: South Beruj fault, Sa: Samalqan.

70 km WNW of Ashkhaneh city (Figure 6a). Numerous streams and rivers show evidence of left-lateral offset along the fault (Figure 6f, 6g). A deflected river with a left-lateral displacement of about 150 m is visible along the fault (Figure 6f).

4. Discussion

In mountain belts, tectonic geomorphology studies yield a unique insight into active faults (Kirby & Ouimet, 2011). The tectonic activity of the Ashkhaneh fault zone is mainly due to the

E-W trending range-parallel reverse faults (Kuh-e-Docheng fault, North Beruj fault, and South Beruj fault) and NE-SW to ENE-WSW trending range-crossing left-lateral strike-slip tear faults. Left-lateral tear faults cutting the Ashkhaneh fault zone influence its morphology conspicuously (Figure 6b-f).

Using the paleomagnetic data, Mattei et al. (2017) presented a geodynamic model for the north and northeast of Iran (Figure 7). Their geodynamic model implies two stages of faulting in the Ashkhaneh fault zone. In the first stage (6-4 Ma), the major E-W trending reverse faults including the Ashkhaneh fault zone developed in response to the collision of Central Iran with the South Caspian Basin (Figure 7a). In the second stage (present-day), the progressive N-S shortening has resulted in mountain curvature in eastern Alborz (Hollingsworth et al., 2010), and the formation of strike-slip tear faults in response to the differential shortening along the Ashkhaneh fault zone (Figure 7b, 7c), like the model presented by Weil et al. (2010) in their investigation on kinematic evolution of curved mountain belts.

Based on the geodetic Global Positioning System (GPS) measurements (Vernant et al., 2004; Khorrami et al., 2019), in the present-day kinematics, the overall Arabia-Eurasia motion (black arrows in Figure 8c) changes along the strike of the Ashkhaneh fault. The GPS station (St01) in the south of the Ashkhaneh fault zone, and the GPS station (St02) in the north of the Ashkhaneh fault (Figure 8a) show northward and northwestward motion with respect to Eurasia, respectively. The difference in the convergence between northern and southern areas of the Ashkhaneh fault zone appeared as different fault-perpendicular velocities along the strike of the fault zone (red arrows in Figure 8c), led to left-lateral movements (Blue arrows in Figure 8c) on Ashkhaneh fault zone. This is consistent with morphotectonic evidence (uplifted surfaces, left laterally offset streams, and rivers) along the fault (Figure 5b-5e). It is noteworthy that the Ashkhaneh fault zone is not the only structure located between GPS stations St01 and St02; therefore, all the obtained lateral displacements in Figure (8c) are not due to a sinistral displacement along the Ashkhaneh fault zone. For instance, the Cheshmeh Nik reverse sinistral fault (Figure 2) located almost north of the St01

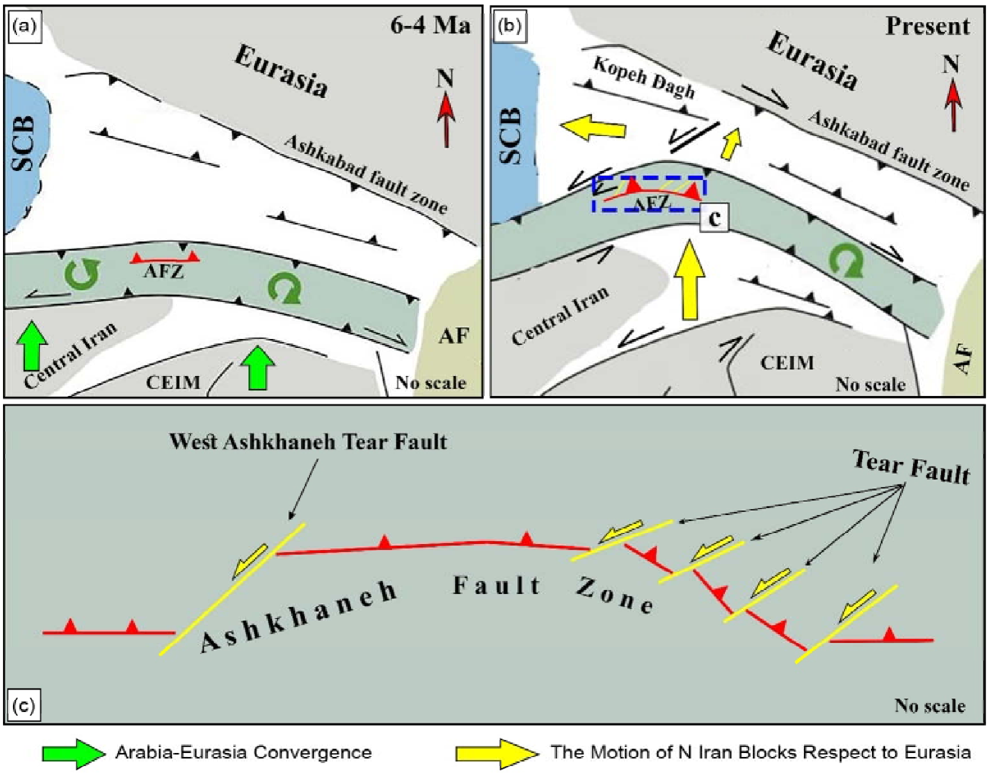

Figure 7. Schematic cartoon of the tectonic evolution of Northeastern Iran from 6 Ma to present (modified from Mattei et al. 2017) (a and b), and map of Ashkhaneh fault zone (c). SCB: South Caspian Basin, AF: Afghanistan, CEIM: Central-East Iranian Microcontinent, AFZ: Ashkhaneh fault zone.

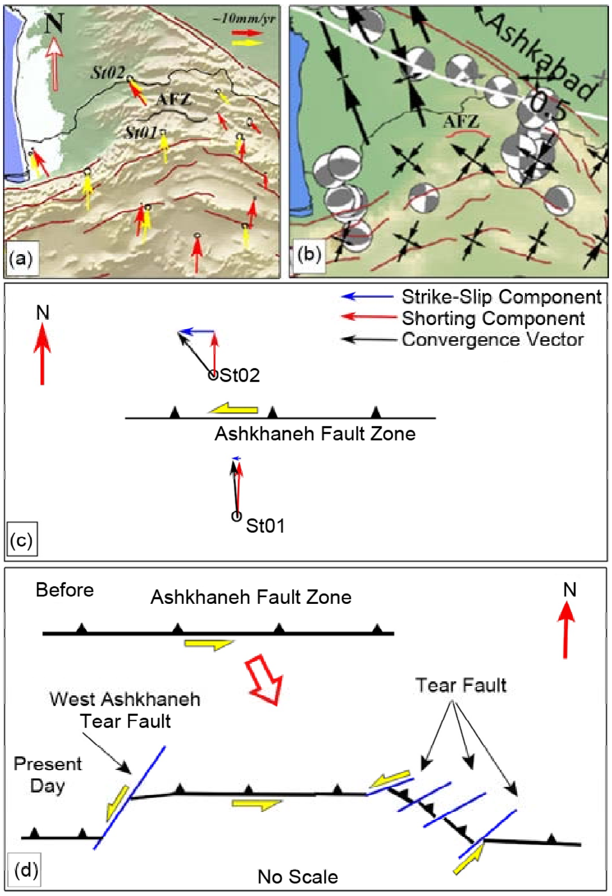

Figure 8. (a) GPS-derived velocity field for the NE Iran, with respect to stable Eurasia reference frame (Khorrami et al., 2019). The yellow and red arrows represent the GPS-estimated movement of the Arabian plate relative to the Eurasian plate. AFZ: Ashkhaneh fault zone. (b) Strain-rate tensor using the velocity field shown in Fig. 8a at the scale of Iran (Khorrami et al., 2019). (c) Partitioning of convergence (black arrows) via shortening (red arrows) on thrusts combined with right-lateral strike-slip (blue arrows). (d) Schematic cartoon of the Ashkhaneh fault zone evolution.

contributes to strain accommodation as well (Mousavi et al., 2013, 2015). Gholami et al. (2017) argued that north-dipping thrust faults in the hanging-wall of the Ashkhaneh fault zone (e.g., North Beruj and South Beruj faults) are evidence of the greater convergence in the east than in the west part of the Ashkhaneh fault zone. Such differences in convergence movement (causing different strain-rates) between the western and eastern parts of the Ashkhaneh fault zone may lead not only to change in the strike of the Ashkhaneh fault, but also in the formation of tear faults and their left-lateral movements (Figure 8d).

Large earthquakes related to tear fault ruptures have been reported around the world. The 2003 Zemmouri (M_w 6.8) at the eastern edge of the Tibetan plateau, and the 2008 Wenchuan (M_w 7.9) earthquakes in the Algiers region are well-known examples of tear faulting events (Belabbes et al., 2009; Feng et al., 2017; Akoglu et al., 2018). Examples of $M \geq 5.0$ earthquakes related to tear faults in Iran are shown in Figure (9).

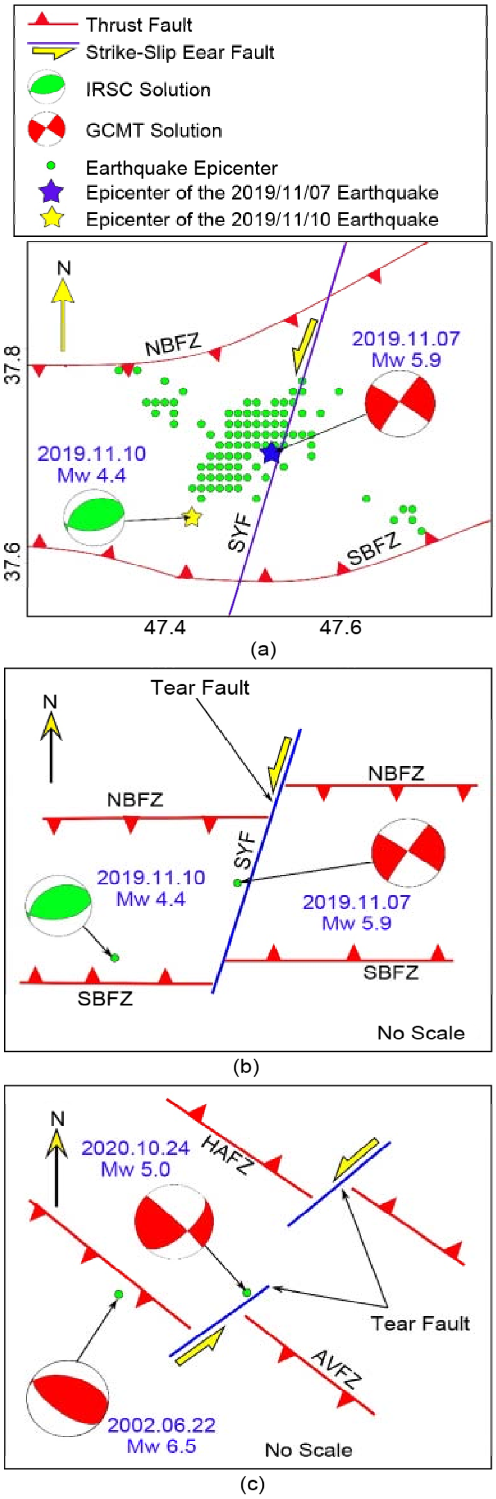

Figure 9. Epicenter distribution map of earthquakes ($2.5 \leq M_N \leq 4.8$) recorded by the IRSC from 2019/11/07 to 2020/02/30 (a). Seismicity on tear faults in Northwestern Iran (b), and Avaj region in the west of Alborz belt (c). SBFZ: South Bozgoush fault zone, NBFZ: North Bozgoush fault zone, SYF: Shalgun-Yelimsi fault zone, AVFZ: Avaj fault zone, HA.

The 2019/11/07, Mw 5.9 Turkmanchai earthquake in northwestern Iran that caused over 100 fatalities and extensive damages, mainly in the Turkmanchai region, took place on the NE-SW trending left-lateral strike-slip tear fault of about 25 km length within the Bozgush Mountains (Valerio et al., 2020). Based on the Inversion of Sentinel-1 DInSAR Measurements, Valerio et al. (2020) proposed an active NE-SW trending left-lateral strike-slip fault as a possible source of the 2019/11/07 earthquake. However, Isik et al. (2021) point to dextral WNW-ESE trending right-lateral strike-slip faults within the Bozgush Mountains, where the 2019/11/07 earthquake occurred. From 2019/11/07 to 2020/02/30, the mainshock was followed by more than 185 events with $2.5 \leq M_N \leq 4.8$, as recorded by the Iranian Seismological Center (IRSC) (Figure 9a). The aftershocks of the 2019/11/07 Turkmanchai earthquake represent a NE-SW direction that is consistent with the geometry of the Shalgun-Yelimsi fault. Near vertical NE-SW nodal plane in the focal mechanism solution of the Turkmanchai earthquake seems consistent with the location of the mainshock and its aftershocks; although, the location error in a range of a few kilometers is inevitable (Figure 9a and 9b). The 2020/10/24, Mw 5.0 earthquake in the Avaj region took place on an E-W trending range-crossing left-lateral tear fault of about 5 km length (Figure 9c). Tear faults in the Ashkhaneh fault zone seem similar to that of the Bozgush Mountains and Avaj region, considering the length (5 to 25 km) and sense of slip (left-lateral motion). Although no earthquakes with $M \geq 5.0$ have been recorded on or near the tear faults of the Ashkhaneh fault zone during the instrumental time-period, such tectonic similarity may imply the potential of these tear faults to cause moderate-magnitude earthquakes.

In seismically active regions, fault interaction is an important and key issue for detailed seismic hazard assessments (Ghassemi et al., 2014; Peacock et al., 2017; Feng et al., 2017, Akoglu et al., 2018, Valerio et al., 2020). The geometry of active faults may provide insights into interactions between fault structures as well as potential locations of future-triggered earthquakes (Berberian, 2014). Similar to the earthquake occurrences on the Shalgun-Yelimsi tear fault (2019/11/07, M_w 5.9) and South Bozgush thrust fault (2019/11/10, M_w 4.4) in northwestern Iran (Figure 9b); and possibly the Avaj thrust fault zone and its tear fault (Figure 9c), the E-W trending Ashkhaneh thrust fault and NE-SW to ENE-WSW trending strike-slip tear faults in this fault zone seem to have interactions, so that movement along one of these faults may cause activation of the other fault. This is an important and key issue for detailed seismic hazard assessments.

5. Conclusion

The Ashkhaneh Fault zone is an active thrust fault system in the western Kopeh-Dagh mountain range, NE Iran, dissected by a number of NE-SW to ENE-WSW trending sinistral strike-slip tear faults with marked displacements. The Ashkhaneh fault zone has been developed in response to the N-S-oriented shortening between the central Iran microcontinent and Eurasia. The Ashkhaneh fault and its related tear faults, formed in response to differential shortening along the fault zone, seem to have interactions, so that the likely movement on one of these faults will lead to movement in another fault(s), similar to the experience of earthquakes on the Shalgun-Yelimsi tear fault and south Bozgush thrust fault in northwestern Iran.

References

Akoglu, A.M., Jonsson, S., Wang, T., Dakir Z., & Dogan U. et al. (2018). Evidence for tear faulting from new constraints of the 23 October 2011 M_w 7.1 Van, Turkey, earthquake based on InSAR, GPS, coastal uplift, and field observations. *Bulletin of the Seismological Society of America*, *108*, 1929-1946.

Ambraseys, N.N., & Melville, C.P. (1982) *A History of Persian Earthquakes*. Cambridge University Press, Cambridge, 219 p.

Belabbes, S., Wicks, C., Cakir, Z., & Meghraoui, M. (2009). Rupture parameters of the 2003 Zemmouri (Mw 6.8), Algeria, earthquake from joint inversion of interferometric synthetic aperture radar, coastal uplift, and GPS. *Journal of Geophysical Research*, *114*, B03406.

Berberian, M. (1981). 'Active faulting and tectonics of Iran: in Zagros Hindukush-Himalaya Geodynamic evolution', Gupta, H.K. and Delany, F.M. (eds.), Am. Geophys. *Union and Geol. Soc. Am., Geodyn. Ser.*, *3*, 33-69.

Berberian, M. (2014). *Earthquakes and Coseismic Faulting on the Iranian Plateau: A Historical, Social and Physical Approach*. Elsevier Series Development in Earth Surface Processes 17, Amsterdam, the Netherlands, 776 pp.

Berberian, M., & Yeats, R.S. (1999). Patterns of historical earthquake rupture in the Iranian Plateau. *Bulletin of the Seismological Society of America*, *89*, 120-139.

Bretis, B., Grasemann, B., & Conradi, F. (2012). An active fault zone in the Western Kopeh-Dagh (Iran), Austrian. *Journal of Earth Sciences*, *105*, 95-107.

Fattahi, M., Walker, R., Hollingsworth, J., Bahroudi, A., Nazari, H., Talebian, M., Armitage, S., & Stokes, S. (2006). Holocene slip rate on the Sabzevar thrust fault, NE Iran determined using optically stimulated luminescence (OSL). *Earth and Planetary Science Letters*, *245*, 673-684.

Feng, G., Jonsson, S., & Klinger, Y. (2017). Which fault segments ruptured in the 2008 Wenchuan earthquake and which did not? New evidence from near-fault 3D surface displacements derived from SAR image offsets. *Bulletin of the Seismological Society of America*, *107*, 1185-1200.

Ghassemi, M.R., Fattahi, M., Landgraf, A., Ahmadi, M., Ballato, P., & Tabatabaei, S.H. (2014). Kinematic links between the Eastern Mosha Fault and the North Tehran Fault, Alborz range, northern Iran. *Tectonophysics*, *622*, 81-95.

Ghayournajarkar, N., & Fukushima, Y. (2020). Determination of the dipping direction of a blind reverse fault from InSAR: case study on the 2017 Sefid Sang earthquake, northeastern Iran. *Earth, Planets and Space*, *72*, 64, https://doi.org/10.1186/s40623-020-01190-6.

Gholami, E., Shoraka, S., & Yassaghi, A. (2017). Structural evolution of Ashkhaneh fault zone in northwestern Kopeh-Dagh (NE Iran). *Scientific Quarterly Journal, GEOSCIENCES*, *26*, *104*, 163-172 (in Farsi).

Hollingsworth, J., Fattahi, M., Walker, R., Talebian, M., Bahroudi, A., Bolourchi, M.J., Jackson, J., & Copley, A. (2010). Oroclinal bending, distributed thrust and strike-slip faulting, and the accommodation of Arabia-Eurasia convergence in NE Iran since the Oligocene. *Geophysical Journal International*, *181*, 1214-1246.

Hollingsworth, J., Jackson, J., Walker, R., & Nazari, H. (2008). Extrusion tectonics and subduction in the eastern South Caspian region since 10 Ma. *Geology*, *36*, 763-766.

Hollingsworth, J., Jackson, J., Walker, R., Gheitanchi, M., & Bolourchi, M. (2006). Strike-slip faulting, rotation, and along-strike elongation in the Kopeh-Dagh mountains, NE Iran. *Geophysical Journal International*, *166*, 1161-1177.

Isik, V., Saber, R., & Caglayan, A. (2021). November 08, 2019 Turkmanchay earthquake (Mw: 5.9) in NW Iran: an assessment of the earthquake using DInSAR time-series and field evidence. *Natural Hazards*, *105*, 3013-3037.

Jackson, J., Haines, J., & Holt, W. (1995). The accommodation of Arabia-Eurasia Plate convergence in Iran. *Journal of Geophysical Research*, *100*, 205-215.

Javidfakhr, B., Bellier, O., Shabanian, E., Siame, L., Benedetti, L., Braucher, R., Bourlès, D., & Abbassi, M.R. (2009). Active tectonic analysis of the Ashkhaneh fault in western Kopeh-Dagh (Iran). Congrès des Doctorants en Sciences de l'Environnment (31 Mars au 1er Avril), Marseille, 78pp.

Javidfakhr, B., Bellier, O., Shabanian, E., Siame, L., Léanni, L., Bourlès, D., & Ahmadian, S. (2011). Fault kinematics and active tectonics at the southeastern boundary of the eastern Alborz (Abr and Khij fault zones): geodynamic implications for NNE Iran. *Journal of Geodynamics*, *52*, 290-303.

Khorrami, F., Vernant, Ph., Masson, F., Nilfouroushan, F., Mousavi, Z., Nankali, H., Saadat, S.A., Walpersdorf, A., Hosseini, S., Tavakoli, P., Aghamohammadi, A., & Alijanzade, M. (2019). An up-to-date crustal deformation map of Iran using integrated campaign-mode and permanent GPS velocities. *Geophysical Journal International*, *217*, 832-843.

Kirby, E., & Ouimet, W. (2011). Tectonic geomorphology along the eastern margin of Tibet: insights into the pattern and processes of active deformation adjacent to the Sichuan Basin. *Geological Society of London, Special Publications*, *353*, 165-188.

Lin, N., Stein, R. S., Meghraoui, M., Toda, S., Ayadi, A., Dorbath, C., & Belabbes, S. (2011). Stress transfer among en echelon and opposing thrusts and tear faults: Triggering caused by the 2003 $M_w = 6.9$ Zemmouri, Algeria earthquake. *Journal of Geophysical Research*, 116, B03305.

Mattei, M., Cifelli, F., Alimohammadian, H., Rashid, H., & Winkler, A., & Sagnotti, L. (2017). Oroclinal bending in the Alborz Mountains (Northern Iran): new constraints on the age of South Caspian subduction and extrusion tectonics. *Gondwana Research*, *42*, 13-28.

Mirzaei, N., Gao, M., & Chen, Y.T. (1998). Seismic source regionalization for seismic zoning of Iran: major seismotectonic provinces. *J. Earthquake Prediction Research*, *7*, 465-495.

Mirzaei, N., Gheitanchi, M. R., Naserieh, S., Raeesi, M., Zarifi, Z., & Tabaei, S. G. (2002). *Basic Parameters of Earthquakes in Iran*. Daneshnegar Pub., Tehran, 185 pp.

Mousavi, Z., Pathier, E., Walker, R.T., Walpersdorf, A., Tavakoli, F., Nankali, H., Sedighi, M., & Doin, M. (2015). Interseismic deformation of the Shahroud fault system (NE Iran) from space-borne radar interferometry measurements. *Geophysical Research Letters*, *42*, 5753-5761.

Mousavi, Z., Walpersdorf, A., Walker, R.T., Tavakoli, F., Pathier, E., Nankali, H., Nilfouroushan, F., & Djamour, Y. (2013). Global positioning system constraints on the active tectonics of NE Iran and the South Caspian region. *Earth and Planetary Science Letters*, 377-378, 287-298.

Peacock, D.C.P., Nixon, C.W., Rotevatn, A., Sanderson D.J., & Zuluaga, L. F. (2017). Interacting faults. *Journal of Structural Geology*, *97*, 1-22.

Prajapati, S., & Mishra, O.P. (2021). Co-seismic deformation and slip distribution of 5 April 2017 Mashhad, Iran earthquake using InSAR sentinel-1A image: implication to source characterization and future seismogenesis. *Natural Hazards*, *105*, 3039-3057.

Qingfen, M., Zhaohui, X., & Huaimin et al. (2008). Characteristics and controlling over reservoir accumulation of tear fault in foreland thrust belt of Baikouquan area in the northwestern margin of Junggar Basin. *Journal of China University of Petroleum*, *32*, 18-27.

Shabanian, E., Bellier, O., Siame, L., Arnaud, N., Abbassi, M., & Cocheme, J. (2009). New tectonic configuration in NE Iran: active strike-slip faulting between the Kopeh-Dagh and Binalud mountains. *Tectonics*, *28*, TC5002.

Tchalenko, J.S. (1975). Seismicity and structure of the Kopet Dagh (Iran, USSR). *Phil. Trans. R. Soc. Lond., Series A.*, *278*, 1-28.

Twiss, R.J., & Moores, E.M. (2007). *Structural Geology*. 2nd ed., W.H. Freeman and Company, New York, 742 pp.

Valerio, E., & Manzo et al. (2020). Seismogenic Source Model of the 2019, M_w 5.9, East-Azerbaijan Earthquake (NW Iran) through the Inversion of Sentinel-1 DInSAR Measurements, remote sensing, *12*, 1346.

Vernant, P., Nilforoushan, F., Hatzfeld, D., Abbassi, M.R., Vigny, C., Masson, F., Nankali, H., Martinod, J., Ashtiani, A., Bayer, R., Tavakoli, F., & Chéry, J. (2004). Present-day crustal deformation and plate kinematics in the Middle East constrained by GPS measurements in Iran and northern Oman. *Geo-physical Journal International*, *157*, 381-398.

Weil, A. B., Yonkee, A., & Sussman, A. (2010). Reconstructing the kinematic evolution of curved mountain belts: A paleomagnetic study of Triassic red beds from the Wyoming salient, Sevier thrust belt, U.S.A. *Geological Society of America*, *122*, 3-23.

Xue, Y., & Wang et al. (2021). Development characteristics and petroleum geological significance of tearing faults in Hashan area. *6th International Conference on Energy Science and Applied Technology, Earth and Environmental Science*, *804*, 022032.

Yong, W. (2010). Study on tearing fault of Keshang formation reservoir in Bai21 well area. *Journal of Oil and Gas Technology*, *32*, 211-213.

Yong, Y., Liangjie, T., & Tengxiao et al. (2014). Deformation characteristics and formation mechanism of tear faults in Yubei 3D area, Tarim basin. *Journal of China University of Mining and Technology*, *43*, 442-447.